

## PREDICTIVE MODELING FOR FOULING AND CLEANING IN HEAT EXCHANGERS DURING MILK PASTEURIZATION

\* Deniz Yilmaz<sup>1,2</sup>, Khoang Kyong Nguen<sup>1</sup>, Mahieddine Chergui<sup>1</sup>, Heni Dallagi<sup>2</sup>, Guillaume Delaplace<sup>2</sup>

<sup>1</sup> THRASOS AI, R&D Department, St Malo, France

<sup>2</sup> University of Lille, CNRS, INRAE, Centrale Institute, UMR 8207 - UMET - Unité Matériaux et Transformations, Lille, 59000, France

### ABSTRACT

In the dairy industry, heat exchangers are essential for milk pasteurization, a process frequently compromised by fouling, which diminishes heat transfer efficiency and affects product quality. Addressing the challenges of fouling and subsequent cleaning is pivotal for ensuring the safety and operational efficiency of pasteurization processes. Our research introduces a comprehensive approach through the development of a predictive fouling model paired with a dynamic cleaning model, aimed at overcoming these obstacles.

The predictive fouling model, which forecasts the separate masses of protein and mineral fouling on heat exchanger surfaces during milk pasteurization, synthesizes two distinct models previously proposed in the literature but never before integrated. This model integrates hydrodynamics, denaturation, and deposition kinetics, along with process characteristics to provide an accurate prediction. Additionally, a dynamic cleaning model was also established to track the transition of the initial deposit mass through an intermediate state before removal, enabling the optimization of cleaning times. This model considers key physico-chemical parameters such as temperature, concentration, and circulation rate of the cleaning agents, to predict and minimize cleaning times for both alkaline and acid solutions effectively.

Preliminary validation studies with industrial partners confirmed the accuracy of the predicted fouling mass per area and the efficacy of cleaning with the proposed dynamic model. Pasteurization experiments at 80°C for 5 hours with a flow rate of 22.7m<sup>3</sup>/h demonstrated the model's precision in estimating total deposit mass and the ratio of inorganic/organic components, consistent with the literature. This predicted deposit mass was further employed to revisit cleaning times for both acid and

alkaline cleaning, and the efficacy of the predicted cleaning sequences has been successfully validated.

This research marks a significant advancement in the predictive management of fouling and cleaning in milk pasteurization, offering both theoretical insights and practical solutions to enhance operational efficiency and product safety.

### INTRODUCTION

Clean-In-Place (CIP) systems are indispensable in maintaining the hygiene of processing lines and ensuring the safety of food products within the agro-food industry. Despite their crucial role, these cleaning operations contribute significantly to water and energy consumption (steam and electricity), generating substantial volumes of wastewater, including environmentally aggressive chemical detergents, accounting for up to 80% of industrial effluent directed to treatment plants (Van Asselt et al., 2005). To reduce the risk of product contamination on processing lines, cleaning sequences (pre-rinsing, alkaline cleaning, acid cleaning, and final rinsing) often remain oversized, despite their significant annual budgets and considerable negative impacts on the environment (Zouaghi et al., 2019).

To face these fouling drawbacks, a lot of effort has been devoted to the scientific community to demystify fouling. Fouling, defined as the unwanted accumulation of material on a surface from a product flow (Wilson, 2018), is a common issue in the food industry. The non-exhaustive list of fouling-related issues commonly encountered in the food industry proposed by Goode et al. (2013) well reflects the breadth of this theme. In the agro-food context, fouling becomes even more crucial as it challenges the quality, and hygiene of processing lines, and segues food safety issues (Zouaghi, 2018).

Particularly in dairy processing, fouling layers typically hydrated and rich in nutrients, provide favorable locations for the colonization of

pathogenic or spoilage microorganisms if not adequately cleaned (Goode et al., 2013). Investigations on milk fouling have allowed to categorization of milk deposits into Type A and Type B, distinguished by the temperature ranges during treatment (Lyster, 1965, Burton, 1959). Type A deposits form between 75 and 110 °C, comprising 50 to 70% proteins and 30 to 50% minerals, while Type B deposits form between 110 and 140 °C, consisting of 15 to 20% proteins and 70 to 80% minerals.

Moreover, the key phenomena of milk fouling modeling have always been the denaturation of  $\beta$ -lactoglobulin. De Jong's predictive fouling model from the nineties was an early success in industrial applications (De Jong, 1992). Subsequent studies such as Petit et al. (2011), Khaldi et al. (2016), and Liu et al. (2022a), have further investigated protein fouling mechanisms during whey protein pasteurization and pointed out that mineral role in dairy derivative deposit formation, especially calcium, should not be neglected. In the same sense, Liu et al. (2021) have shown that casein modifies both  $\beta$ -lactoglobulin interactions and mineral equilibrium compared to casein-free dairy derivatives.

Various fouling models have been proposed for milk derivatives. These models help translate lab and pilot plant data into insights for industrial-scale applications (Benning et al., 2003, Alhuthali 2022, Liu 2022b). Once validated, these models enable the estimation of the optimal temperature-time profiles for heated products, minimizing fouling while ensuring food safety standards (De Jong, 1996).

Despite the availability of predictive models for milk fouling, a notable gap exists in the literature regarding the integration of this crucial information into predicting cleaning kinetics and optimizing CIP sequences based on deposit mass and composition. To effectively model milk fouling for industrial cleaning purposes, both organic and inorganic fouling must be considered. Most research primarily describes deposits resulting from pasteurization treatment as solely an accumulation of proteinaceous material, with little consideration for minerals.

However, the literature also acknowledges the kinetics of mineral formation in fouling studies (Spanos et al, 2007; Tung, 1998; Eliaz & Sridh, 2008; Barone, 2021). Calcium salts, particularly calcium phosphate, are identified as the primary minerals contributing to fouling in milk. However, in complex solutions like milk, predicting the behavior of calcium salts under heat is challenging. Spanos et al.'s work also highlights a notable gap in the literature on heat exchanger fouling, which often underemphasizes the precipitation mechanism of calcium phosphate in dairy solutions (Spanos et al, 2007).

Addressing this gap, this study introduces an innovative numerical methodology aimed the optimization of traditional CIP programs within the dairy sector, taking advantage of deposit fouling mass predicted by pasteurization treatment. This methodology distinctively integrates both acid and alkaline cleaning sequences, leveraging advanced predictive models to tailor cleaning processes with precision. The alkaline cleaning protocols are refined by better understanding the initial mass of organic fouling during milk heat treatment. Simultaneously, insights into the initial mass of inorganic deposits provide precise guidance for optimizing acid cleaning times. The basis of this research is the novel juxtaposition of two models: the first model predicts the intricate dynamics of protein and mineral deposit formation on heat exchanger surfaces, while the second anticipates their efficient removal during milk's thermal processing. This dual-model framework, forecasting both the deposition and removal of protein and mineral deposits, represents a significant advancement.

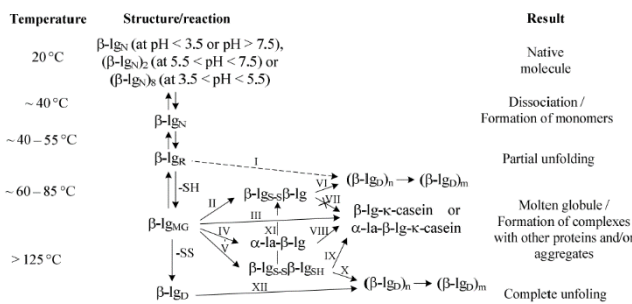
## MATERIAL AND METHODS

### PREDICTIVE PROTEIN FOULING MODEL

Whey proteins are the most thermosensitive components of milk, leading to their predominant presence in deposits generated by thermal processes (Tuoc, 2015). However, not all these proteins respond to heat in the same way. Polat (2009) reports that alpha-lactalbumin ( $\alpha$ -La) has the lowest denaturation temperature, followed by bovine serum albumin (BSA), immunoglobulins, and finally, beta-lactoglobulin ( $\beta$ -Lg).  $\beta$ -Lg exhibits faster denaturation kinetics than other proteins in the typical temperatures of pasteurization due to its low thermal stability and structural characteristics, making it the predominant protein found on fouled surfaces (Sadeghinezhad et al., 2014). Moreover, a correlation has been established between the denaturation kinetics of  $\beta$ -Lg and fouling growth (Dalglish, 1990, Blanpain-avet et al. 2016). This protein is, therefore, the focus of numerous studies on milk fouling (Journink et al., 1996; Jimenez et al., 2013; Khaldi et al., 2018). As shown in Figure 1., as the temperature rises,  $\beta$ -Lg successively loses its quaternary (dimer association) and tertiary structures, becoming capable of associating with other denatured  $\beta$ -Lg molecules or surfaces to form tenacious fouling. It is considered that above 60°C, the disruption of weak intramolecular bonds leads the protein to a "molten globule" state, reversible at this stage. Beyond 80°C,  $\beta$ -Lg is irreversibly denatured due to the rupture of intramolecular covalent bonds (including disulfide bridges), and above 130°C, it loses its secondary structure. The

rate of denatured  $\beta$ -Lg is highly complex and depends on environmental conditions such as pH (Westhoff, 1978), heating conditions (temperature, heating rate, duration), protein and mineral concentrations, ionic strength, and hydrodynamic conditions (Boxler, 2014; Khaldi, 2016). Calcium's influence is particularly crucial for the denaturation/aggregation phenomenon, as an increase in calcium concentration, has been shown to decrease the denaturation temperature of  $\beta$ -Lg from 83°C to 75°C (Xiong, 1992). Petit et al. (2011) have also highlighted the catalytic effect of calcium on the denaturation and aggregation kinetics of  $\beta$ -Lg. The kinetic pathway (Figure 1) can be mathematically expressed as a consecutive sequence of unfolding (N to U), aggregation (U to A) reactions as shown in equations 1,2,3,4, and 5 (de Wit and Klarenbeek, 1989), and deposition. The application of the model, based on empirical kinetic data concerning the unfolding and aggregation of  $\beta$ -LG, can be utilized in thermal denaturation. In this scenario, N, U, A, and D represent the native, unfolded, aggregated, and deposited states of  $\beta$ -LG,

Jun and Puri (2005, 2006) present a methodology for 3D modeling of beta-lactoglobulin fouling in a plate heat exchanger for milk using Computational Fluid Dynamics (CFD) with FLUENT software. The CFD model addresses 3D flow equations, species transport modeling, and deposition rate calculations. They visualized velocity profiles at different channel locations, simulated fluid milk temperature profiles on the plate surface, and calculated heat transfer area and flux to determine protein unfolding, aggregation rates, and wall deposition. The authors rely on the theory that only unfolded proteins deposit on the walls. This thermal modeling theoretically calculates the beta-lactoglobulin population balance (unfolded, aggregated, and deposited species) of the protein at all points but practically on the mesh points of the system, according to the Arrhenius equation (Equations 1.2.3.4), characterizing the fouling deposition at time t. Their predicted mass deposit values were in good agreement with the experimental data, with a prediction error of 0.01 g. According to their results, their model successfully couples the hydrodynamic and thermodynamic performances of PHEs with chemical reaction equations for protein denaturation and absorption onto the stainless-steel surface.



In this work, a similar was adopted to get the organic part of fouling in milk, drawing inspiration from Jun and Puri's methodology (2005, 2006). COMSOL Multiphysics was employed as the Computational Fluid Dynamics (CFD) software. The CFD model, like theirs, tackled the 3D flow equations, species transport modeling, and deposition rate calculations. By drawing on their approach, we introduce several key improvements and novel applications that significantly advance the field. Importantly, we adapt our model to consider the specific composition, physicochemical, and thermal properties of milk. This tailored approach allows us to explore the complex interactions between fluid dynamics, heat transfer, and protein denaturation kinetics. Through this focused analysis, we uncover critical factors influencing fouling deposition and develop customized strategies to mitigate fouling in milk processing PHEs.

respectively.

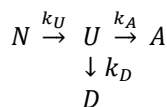


Fig. 1. Mechanisms of thermal denaturation for why protein solutions and their potential interactions (Boxler, 2014):  $\beta$ -Lg N: native /  $\beta$ -Lg R: native reversible /  $\beta$ -Lg MG: molten globule /  $\beta$ -Lg D: denatured.

$$-\frac{dC_N}{dt} = k_U C_N \quad (1)$$

$$-\frac{dC_U}{dt} = k_U C_N - k_A C_U^2 - k_D C_U \quad (2)$$

$$-\frac{dC_A}{dt} = k_A C_U^2 \quad (3)$$

$$-\frac{dC_D}{dt} = k_D C_U \quad (4)$$

$$k_i = k_{0i} e^{-\frac{E_i}{RT}} \quad (i = N, U, A \text{ and } D; T, K) \quad (5)$$

### PREDICTIVE MINERAL FOULING MODEL

Certain models of protein deposit formation consider the calcium content to explain an increase in deposits and others modify the constants of the denaturation kinetics as a function of the calcium content (Alhuthali, 2022; Khaldi, 2015-2018). However, few models have been proposed to predict fouling due to the precipitation of mineral salts. The literature unanimously designates calcium salts,

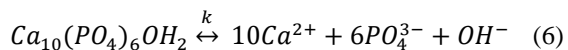
primarily calcium phosphate, as the main minerals in milk contributing to fouling. Calcium salts indeed exhibit solubility inversely proportional to heat (Skudder et al., 1981; Visser and Jeurmink, 1997; Sadeghinezhad et al., 2014).

The precipitation and crystallization of calcium salts are complex processes influenced by the pH and temperature of the medium, even in very simple solutions. In complex solutions like milk, calcium salts can interact with organic species (soluble proteins, caseins, fat globules) or inorganic species (phosphates) to contribute to fouling.

Generally, calcium is considered a key element in milk fouling. In the absence of calcium, fouling is significantly inhibited (Jimenez et al., 2013). Boxler (2014) lists four major effects of calcium that explain, alone or combined, its importance in fouling: (i) Calcium modifies denaturation and aggregation constants, promoting reactivity and thus fouling. (ii) Calcium neutralizes local negative charges on proteins, reducing electrostatic repulsion phenomena and encouraging their aggregation on the deposit. (iii) Calcium allows molecular bridging between the existing deposit and still free fouling precursors. (iv) Nanoclusters of calcium phosphate act as a cement, holding casein micelles and they are temperature sensitive. Consequently, the equilibrium between the serum and colloidal phase keeps changing during heat treatment.

The calcium/phosphate equilibrium system is quite complex, and different phases of calcium phosphate are found in milk deposits, depending on the overall temperature and level of supersaturation. Precipitation occurs when a solution becomes supersaturated with a particular solute, leading to the formation of solid particles or crystals (Spanos et al., 2007;). In this context, the balance between calcium and phosphate levels is crucial, and different calcium phosphate phases may be present in the milk deposits.

Spanos et al. (2007) investigated how pH and temperature affect the spontaneous precipitation of calcium phosphate from simulated milk ultrafiltrate solutions for the pH range of 5.7 to 7.0 and temperatures between 55 to 75 °C. He argues that precipitates were primarily low-crystallinity prisms of hydroxyapatite. Equation 6 shows the chemical reaction for hydroxyapatite precipitation.



The precipitation kinetics described in the study suggest a parabolic dependence between the initial rates of calcium phosphate precipitation and the solution's supersaturation level in accordance with temperature change. (equation 7 and 8)

$$R = k \cdot \sigma^n \quad (7)$$

$$\sigma = \Omega^{(1/18)} - 1 \quad (8)$$

Where  $k$  is precipitation rate constant,  $n$  is growth order,  $\sigma$  is relative supersaturation and  $\Omega$  is supersaturation ratio.

The calculations were done as indicated in detail in Spanos's work (Spanos et al., 2007).

Relative supersaturation can be calculated as a function of the supersaturation ratio. This implies that the more supersaturated the solution is, the faster the precipitation occurs, but the relationship is not linear – instead, it follows a curve that rises sharply and then tapers off. Comparing IAP (ion activity product) to  $K_{sp}$  (Thermodynamic solubility product) allows to determine whether a solution is at equilibrium ( $IAP = K_{sp}$ ), unsaturated ( $IAP < K_{sp}$ ), or supersaturated ( $IAP > K_{sp}$ ) with respect to a particular ionic compound (equation 9).

$$\Omega = IAP/K_{sp} \quad (9)$$

The temperature dependence of the solubility product and ion activity product for the least soluble form of calcium can be defined and computed, as detailed in the work of Eliaz and Sridh (2008). Therefore, the rate of inorganic fouling with respect to its calcium and phosphate balance, could be modelled based on the least soluble form of calcium phosphates where the precipitation rate depends on the degree of supersaturation. In this work, we adopted this approach to get the mineral part of fouling in milk.

## PREDICTIVE CLEANING MODEL

Certain studies have examined the impact of different cleaning temperatures, durations, and chemical concentrations on the removal of milk-based fouling (Avilla-Sierra et al., 2021; Davey et al., 2015; Gilham et al., 1999; Jeurmink and Brinkman, 1994). However, these models do not account for the initial mass of the deposit to be cleaned. In 1984, Gallot Lavallée developed a predictive cleaning model that correlates cleaning time with temperature, detergent concentration, detergent flow rate, and the mass of the deposit to be cleaned (Gallot Lavallée, 1984). The model was based on pilot plant scale pasteurization conditions resembling those in the dairy industry and used a nonrecycled sodium hydroxide cleaning solution. His work covered a range of parameters, including temperatures from 55°C to 95°C, soda concentrations from 0.1% to 3.9% (by mass), and circulation rates from 0.3 m/s to 1.9 m/s. The cleaning process was monitored in line with an optical sensor that detected the turbidity of deposits being removed.

In the model, the cleaning rate (or removal rate) is expressed as follows:

$$R_{cleaning} = k \cdot m_0 \quad (10)$$

$$\log k = -1.01 + 0.27a + 0.2b + 0.1c - 0.67m_0 \quad (11)$$

In equation (10),  $\log k$  (cleaning reaction rate) is expressed as a function of the temperature of the cleaning detergent ( $^{\circ}\text{C}$ ) ( $a$ ), the concentration of NaOH in the cleaning detergent (%wt) ( $b$ ), and mechanical effect, expressed as the velocity of the cleaning detergent (m/s) ( $c$ ), along with a constant coefficient of initial fouling mass ( $\text{kg}/\text{m}^2$ ). Using regression analysis, including a quadratic model, they identified the influence of parameters such as the initial mass of the deposit, temperature, soda/acid concentration, and the circulation rate of the cleaning solution. Each variable was coded for the analysis, and they calculated the regression coefficients for these variables.

The coefficients in Equation 11 represent the respective impacts of temperature, concentration, and velocity on the sodium hydroxide solution. The approach used follows the methodology of Gallot Lavallée, which addresses both mineral and organic cleaning removals. We retained and adapted the form of the equation proposed by Gallot Lavallée to account for temperature, concentration, and mechanical effects (superficial velocity) for NaOH. A separate equation was developed to describe the cleaning rate for mineral deposits using  $\text{HNO}_3$ . The model divides the initial mass of deposits into organic and inorganic components and applies the cleaning removal rates to simulate the cleaning process for both types of soil (Equations 12 and 13).

$$R_{\text{Cleaning,acid}} = k' \cdot m_{0\text{inorganic}} \quad (12)$$

$$\log k' = -1.01 + 0.27a + 0.2b + 0.1c - 0.67m_{0\text{inorganic}} \quad (13)$$

While respecting the influence of these three parameters on the cleaning rate constant, we have altered the coefficients. However, these alterations are proprietary information held by Thrassos and cannot be disclosed.

## FOULING SIMULATIONS

In this research, we incorporated the reaction kinetics of beta-lactoglobulin to model organic fouling in milk, as outlined by Jun and Puri (2005). Similarly, the kinetics for hydroxyapatite, used to model inorganic fouling, were adapted from Spanos (2007). We employed the COMSOL Multiphysics software, Version 6.2, specifically utilizing its Fluid Flow and Chemical Engineering modules, to simulate the thermal and hydraulic phenomena within the system.

COMSOL software effectively models the mixing and transport of various protein species: native, unfolded, aggregated, and deposited proteins. This is achieved through the solution of

conservation equations for momentum (eq14), mass continuity (eq15), turbulence kinetic energy (eq16), dissipation rate (eq17), and reaction sources for each protein component. The equations are as follows:

$$\rho(u\nabla)u = \nabla [-pI + K] + F \quad (14)$$

$$\nabla(\rho u) = 0 \quad (15)$$

$$K = (\mu + \mu_T)(\nabla u + (\nabla u)^T) - \frac{2}{3}(\mu + \mu_T)(\nabla \cdot u)I - \frac{2}{3}\rho kI$$

$$\rho(u\nabla)k = \nabla[(\mu + \frac{\mu_T}{\sigma_k})\nabla k] + P_k + \rho\epsilon \quad (16)$$

$$\rho(u\nabla)\epsilon = \nabla[(\mu + \frac{\mu_T}{\sigma_\epsilon})\nabla\epsilon] + C_{\epsilon 1}(\frac{\epsilon}{k})P_k - C_{\epsilon 2}\rho(\frac{\epsilon^2}{k}), \quad (17)$$

K-epsilon turbulence model has been selected in order to solve two transport equations: one for the turbulence kinetic energy ( $k$ ) and another for the rate of dissipation of turbulence kinetic energy ( $\epsilon$ ), where  $\rho$  is the density of the fluid ( $\text{kg}/\text{m}^3$ );  $u$  is the velocity vector (m/s);  $p$  is pressure (Pa);  $\mu$  denotes the viscosity of the fluid (Pas);  $I$  is a unit vector;  $F$  is the volume force vector ( $\text{N}/\text{m}^3$ ). These equations and appropriate boundary conditions, form a system that can be solved numerically to simulate turbulent flows.

The software accommodates multiple simultaneous chemical reactions, whether occurring in the bulk phase or on wall surfaces. With capabilities for species transport modeling, both with and without reactions, the approach relies on solving transport equations for species mass fractions using a defined chemical reaction mechanism. The source terms in the species transport equations, representing reaction rates, are determined through Arrhenius rate expressions (equations 1,2,3,4,5).

For this study, the heat exchanger plate was designed based on the real data of the plate from Laita (Alfa Laval, Tetraplex C10- SM), with its real dimensions and configuration on AutoCAD.

The following conditions and considerations have been adopted:

1. The product flow was modeled as three-dimensional, in rectangular Cartesian coordinates, turbulent with channel, and incompressible (negligible pressure work and kinetic energy). The viscous heat dissipation is neglected.
2. The minimum and maximum gaps between the plates were 2 mm and 6 mm, respectively.
3. No slip wall is enforced on every solid surface.
4. The milk flow enters the preheating zone at  $56.6^{\circ}\text{C}$  with a native B-LG mass concentration of 3.2 g/l; the auxiliary flow is counter current. Then enters the heating zone at  $72.6^{\circ}\text{C}$ . The outlet gauge pressure is set to 0 Pa.
5. Preheating and heating zones were simulated separately.

A regular, structured grid of tetrahedral mesh elements was created, and the total number of elements was 1099704. Mesh quality and independence were rigorously assured. The key geometrical specifications and operating conditions for the PHE system are listed in Table 1.

Table 1. Geometrical specification and operating condition for the heating zone of PHE system

Plate model	Tetraplex C10-SM
Material	Stainless Steel 316
Average thickness of the fluid domain (mm)	4
Thickness of the plate (mm)	0.6
Inlet temperature (°C)	72.6
Outlet temperature (°C)	80
Flow rate (m <sup>3</sup> /s)	0.00625/16 <sup>a</sup>
Total number of passes	16

<sup>a</sup> Number of passes

Physicochemical parameters of milk used to simulate 3D fouling are taken from de Jong et al, and added as a function of temperature as shown below.

$$\mu = (0.00445 \cdot T + 0.947) \cdot 10^{-3} \quad (\mu, \text{Pa.s}; T, ^\circ\text{C}) \quad (18)$$

$$\rho = 1033.7 - 0.22308 \cdot T - 0.00246 \cdot T^2 \quad (\rho, \text{Kg.m}^{-3}; T, ^\circ\text{C}) \quad (13)$$

$$C_p = 2.976 \cdot T + 3692 \quad (C_p, \text{J.}^\circ\text{C}^{-1}\text{Kg}^{-1}; T, ^\circ\text{C}) \quad (19)$$

Mineral fouling was calculated based on Spanos et al., specifications. Hydroxyapatite precipitation is modeled to calculate the inorganic fouling mass per area, considering its low solubility. The reaction rate of hydroxyapatite precipitation has a parabolic dependence on the solution supersaturation that is described in equation 7 8 9. Reaction rate order,  $n$ , was reported to range between 2.31 and 2.50 (Spanos et al., 2007). These findings were in accordance with a surface diffusion-controlled mechanism, which is typical for a number of sparingly soluble salts. Therefore, the reaction rate order has been taken as 2.31. Ion activity product calculations were done as a function of active ion concentration and the outlet temperature of each pass as described below (Baron, 2021):

$$IAP = \alpha_{Ca^{2+}}^{10} \cdot \alpha_{Po_4^{3-}}^6 \cdot \alpha_{OH^-}^2 \quad (20)$$

$$\alpha_i = \gamma_i \cdot C_i \quad (21)$$

$$\gamma_i = A \cdot z^2 \left( \frac{\sqrt{I}}{1 + \sqrt{I}} - 0.2 I \right) \quad (22)$$

Where A is Debye–Hückel constant; z is charge of the ions; I is ionic strength;  $\alpha_i$ ,  $C_i$  and  $\gamma_i$  are respectively: ionic activity, concentration, and activity coefficient of  $Ca^{2+}$ ,  $Po_4^{3-}$  and  $OH^-$  ions.

$$A = 0.486 + 6.07 \cdot 10^{-4} \cdot T + 6.43 \cdot 10^{-6} \cdot T^2 \quad (A, \text{mol}^{-1/2}\text{Kg}^{1/2}; T, ^\circ\text{C}) \quad (23)$$

Pasteurization duration and temperature, plate characteristics, flow rate; ionic and total concentrations of calcium, phosphate, and pH of the raw milk were taken as initial input for calculations. The procedure taken to implement fouling formation for each zone is summarized below:

Step 1: Begin with the initial configuration of the Plate Heat Exchanger (PHE) at  $t=0$  s, where there's no fouling present, and define the final simulation time as total pasteurization time (5 hours).

Step 2: Solve the governing equations (12)-(15) assuming steady-state conditions to determine the spatial profiles of fluid velocity.

Step 3: Integrate the bulk and surface reactions Equation (1)-(9), and update the time by  $t + \Delta t$ . ( $\Delta t=10$ ,  $0 < t < 180$ ;  $\Delta t=180$ ,  $180 < t < 1620$ ;  $\Delta t=1800$ ,  $1620 < t < 18000$ ).

Step 4: Combine solutions to determine the surface deposition mass ( $\text{kg/m}^2$ ).

Temperature distribution, velocity profile, and fouling simulation results can be found in the results section.

To quantitatively analyze milk deposits, the Plate Heat Exchanger (PHE) system was operated with raw milk for a duration of 5 hours. Following the shutdown of the system, the array of plates was disassembled. The last plate in the heating zone was selected as a representative sample of the system, and the wet fouled mass was collected using a scraper and subsequently weighed. The measured value was then compared to the simulated data obtained through the utilization of the 3D fouling model.

## CLEANING SIMULATIONS AFTER FOULING PREDICTION

After fouling mass calculations, optimum cleaning was simulated based on the cleaning cycles regularly used by Laita (table 2).

Table 2. Laita cleaning parameters

	Concentration (% wt)	Cleaning Temperature (°C)	Cleaning velocity (m/s)	Old cleaning time (s)
Alkaline	0.94	70	1.07	2900
Acid	1.21	50	1.07	1500

## VALIDATION APPROACH

The validation strategy encompasses both numerical simulations and experimental procedures to ensure the accuracy and reliability of our predictive fouling and cleaning models. The experiments were conducted at the Laita/Yffiniac Plant, utilizing the industrial scale pasteurizer system with raw whole milk pasteurized at 80°C for a total duration of 5 hours with a flow rate of 22.7 m<sup>3</sup>/h. The average and maximum velocity was calculated as 0.304 m/s and 1.41 m/s respectively. The average local cell Reynolds number was calculated as 40218.

The pasteurization system consisted of 4 zones:

(i) Preheating zone consists of 39 plates. The total fluid domain is 19 for unpasteurized milk and 19 for pasteurized milk, the flow is divided by 10 and 9 with 1 separator. (ii) Heating zone consists of 65 plates where the total fluid domain is 32 for unpasteurized milk and 32 for hot water, the flow is divided by 16 and 16 with 1 separator (iii) Precooling zone consists of 201 plates. The total fluid domain is 200; 100 for unpasteurized milk and 100 for pasteurized milk, the flow is divided by 40 – 40 – 20 with 3 separators. (iv) Cooling zone consists of 41 plates; the total fluid domain is 40: 20 for unpasteurized milk and 20 for cold water. There is no separator, the flow is not divided. (Tetraplex, model C-10, Alfa Laval, France). Figure 2, Table 1, and Table 2 show the pasteurizer used in the validation study.



Figure 2. Pasteurizer used in the validation study

Table 3. Temperature profile and configuration of the pasteurizer

Section	Flow rate (kg/h)	Type of Fluid	Temperature (°C)	Plate configuration (# of plates)
Heating	22500	Milk	72.6 – 80	16+16
	30000	Hot water	75 – 80.3	16+16
Preheating	16480	Milk	56.5 - 78.5	10+9
	22500	Milk	63.9 – 80	10+9
Precooling	25000	Milk	6.2 -56.5	40+40+20
	22500	Milk	8.7 – 63.9	40+40+20
Cooling	22590	Cold water	2 – 6.4	20
	22500	Milk	4 – 8.7	20

Following a 5-hour production run, the system was rinsed with water, and the pasteurizer was disassembled to inspect the plates for fouling. Fouling material was scraped off for further analysis to identify the main components, with the scraped area and fouling mass being utilized to compute the fouling mass per area, which was found to be 28.68 g/m<sup>2</sup> (24.8 g/m<sup>2</sup> organic fouling, 4.16 g/m<sup>2</sup> inorganic fouling) in the last plate of the heating zone. Based on these findings, an optimized cleaning protocol was calculated and recommended to Laita. Subsequently, the pasteurizer was reassembled, and the new cleaning program was implemented to evaluate its effectiveness. To validate the simulations against real-world outcomes, the simulated results were compared with experimental data, focusing on three critical aspects: (i) visual observation of the plate surfaces for any residual fouling, (ii) protein testing to assess the cleanliness of the surfaces, and (iii) microbial analysis to detect any contamination.

## RESULTS FOULING SIMULATIONS

The total surface of the plate was calculated with COMSOL Multiphysics. To calculate the fouling at each zone, the preheating and heating zones were divided into 2 and simulated as 4 individual plates. Inlet and outlet temperatures were provided by Laita. The temperature profile and configuration of the pasteurizer are shown in Table 3.

For a total of 5h production time, the concentration of aggregated, unfolded, and deposited protein was calculated. The initial native protein concentration was taken as 0.175 mol/m<sup>3</sup>.

Figures 3,4 and 5 show the simulation results for the velocity profile of milk during pasteurization, the temperature distribution of the heating zone, and the fouling mass per area after 5 hours of pasteurization of raw cow milk respectively. The simulation reveals transient temperature and fouling patterns in fluid milk on the plate within the Plate Heat Exchanger (PHE) system. Notably, localized hot zones emerge, particularly at the upper region near the outlet port and the corner opposite the inlet port, where temperature peaks at 80°C. The calculated fouling map, depicted in Figure 5, clearly illustrates the escalating deposition of milk fouling on the plate surface over time and in response to increasing temperatures. While a significant portion of the plate area remains relatively free of foulants, an observable rise in deposition rate occurs, especially in the upper region near the outlet port, as time progresses.

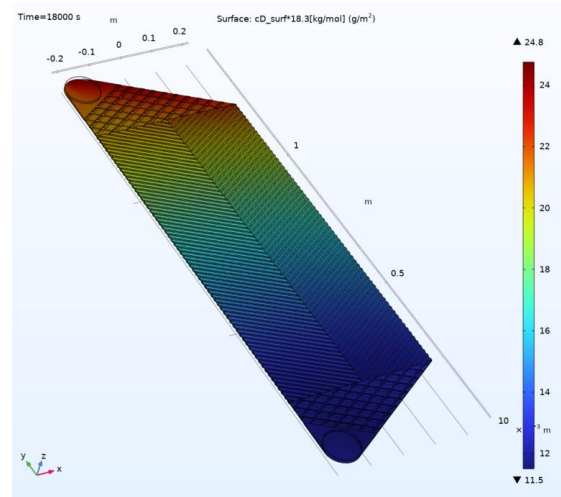


Figure 5. Fouling mass per area ( $\text{g/m}^2$ ) after 5 hours of production

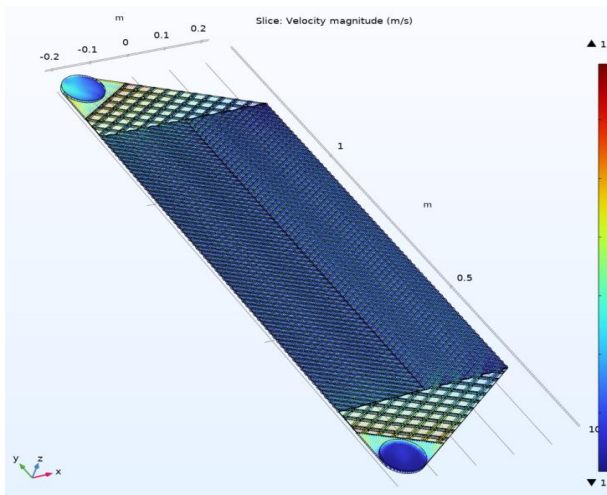


Figure 3. Velocity profile of milk without fouling

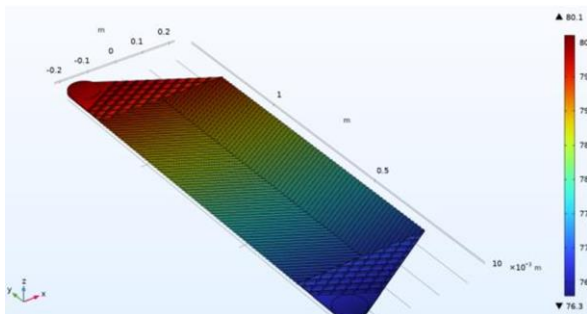


Figure 4. Temperature distribution of the plates in the heating zone

At a pasteurization temperature of 80°C, with specified initial pH and concentrations, the proposed predictive model anticipated a maximum organic fouling of 24.8  $\text{g/m}^2$  and a maximum inorganic fouling of 4.16  $\text{g/m}^2$ . The total fouling predictions achieved a remarkable accuracy level of 99%. The predicted fouling composition revealed an 85% protein ratio and a 15% mineral ratio.

Utilizing the calculated protein and mineral fouling masses, we recalculated the cleaning times for both alkaline and acid cleaning procedures. Although, COMSOL was used for integrating and solving the equations, the specific cleaning calculations were conducted separately using these average parameters. This approach meant that COMSOL was not required for the final cleaning calculations themselves.

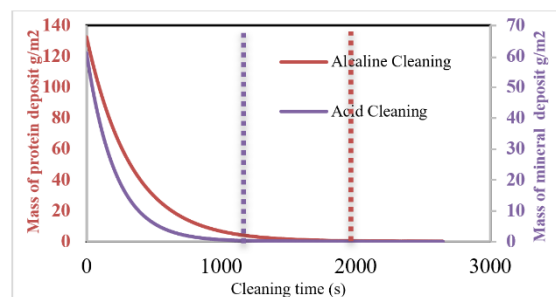


Fig. 6. Cleaning curves and minimum cleaning time determination to eliminate 99.9% inorganic and organic fouling.

The results, presented in Figure 6, illustrate a notable reduction in alkaline cleaning time by 900 seconds, alongside a decrease of 60 seconds in acid cleaning duration in comparison to old cleaning times shown in Table 2. These adjustments reflect not only the precision of the predictive model but also the tangible benefits in terms of operational



efficiency and resource utilization for the cleaning processes.

After implementing the new cleaning time, the pasteurizer underwent dismantling for verification of cleaning efficiency. Visual inspection revealed no residual fouling following the optimized cleaning program. Further protein testing confirmed the cleanliness of the plates, as no protein content was detected in any sample. Microbial analysis conducted by Laita and Thrastos confirmed the absence of microbial contamination on the surface of the plates. The comparative analysis with the previous cleaning times highlighted substantial efficiencies gained by Laita through the optimized alkaline and acid cleaning times. Energy consumption was determined by assessing the power requirements of equipment used in the actual cleaning processes throughout the duration of the optimized Clean-in-Place (CIP) cycle. Notably, the reduction of acid and alkaline cleaning times resulted in significant resource conservation and operational improvements: a reduction of 709 liters in water usage, 1125 liters in wastewater generation, a decrease of 1180 seconds in cleaning duration, and a remarkable 31% reduction in energy consumption. These outcomes underscore the effectiveness and environmental benefits of the optimized cleaning strategy.

## CONCLUSION AND FUTURE WORK

In conclusion, the intersection of food processing economics and environmental concerns underscores the growing significance of employing model-based predictions in addressing fouling removal challenges. This study utilized COMSOL, a computational fluid dynamics software, to simulate the milk fouling and cleaning process in a plate heat exchanger system based on hydrodynamic and thermodynamic principles. The application of such software emerges as a potent tool for predicting process conditions, fouling, and cleaning rates during the pasteurization of milk. The quantitative validation of the model demonstrated a commendable agreement between predicted fouling distribution and the observed experimental outcomes, highlighting the reliability of the simulation.

This research underscores the necessity of advancing mathematical models, specifically addressing thermal protein denaturation and salt precipitation, to better understand fouling growth. While existing fouling models have predominantly focused on the deposition kinetics of  $\beta$ -LG as a mass transfer process governed by chemical reactions, this study represents a novel approach by integrating simultaneous consideration of inorganic and organic

fouling, considering flow characteristics and surface conditions. This integrated modeling approach contributes to a more comprehensive understanding of fouling dynamics in the context of milk pasteurization.

The current deposit formation model, although valuable, has been tested at an industrial scale once in collaboration with our industrial partner and requires further validation with various conditions. It is important to note that the validation was conducted using wet deposits, which could still contain residual moisture. This factor may slightly influence the results, as visually, the deposits appeared dry. Additionally, while other organic deposits may be present in the scraped samples, their quantities are expected to be negligible compared to  $\beta$ -lg. Future studies should consider drying the deposits before validation to ensure a more accurate comparison with the simulation results.

The cleaning model is semi-empirical and demands a broader range of testing conditions for robust validation. Future investigation aims to extend the applicability of these models to different dairy products, and production conditions and expand the cleaning model to encompass a wider array of industrial detergents.

## NOMENCLATURE

$A$	Debye–Hückel constant
$C$	Protein concentration in bulk (mol/m <sup>3</sup> )
$C_A$	Aggregated protein concentration (mol/m <sup>3</sup> )
$C_D$	Deposited protein (mol/m <sup>3</sup> )
$C_N$	Native protein (mol/m <sup>3</sup> )
$C_U$	Deposited protein (mol/m <sup>3</sup> )
$E_a$	Activation energy (J/mol)
$I$	Ionic activity
$IAP$	ion activity product
$k$	Reaction rate
$k_0$	Pre-exponential factor (1/s)
$K_{SP}$	Thermodynamic solubility product
$m_0$	Mass of deposit to be cleaned (kg/m <sup>2</sup> )
$n$	Reaction order
$R$	gas constant (J/mol°C)
$T$	Temperature, °C, °K
$t$	time (s)
$z$	Ionic charge

## GREEK LETTERS

$\alpha_i$	ionic activity concentration
$\gamma_i$	Activity coefficient
$\rho$	Density (kg/m <sup>3</sup> )
$\mu$	Dynamic viscosity (Pa.s)
$\sigma$	Relative supersaturation
$\Omega$	Supersaturation ratio

## REFERENCES

- Alhuthali, S., Delaplace, G., Macchietto, S., & Bouvier, L. (2022). Whey protein fouling prediction in plate heat exchanger by combining dynamic modelling, dimensional analysis, and symbolic regression. *Food and Bioprocess Processing*, 134, 163-180.
- Avila-Sierra, A., Huellemeier, H. A., Zhang, Z. J., Heldman, D. R., & Fryer, P. J. (2021). Molecular Understanding of Fouling Induction and Removal: Effect of the Interface Temperature on Milk Deposits. *ACS Applied Materials and Interfaces*, 13(30), 35506–35517. <https://doi.org/10.1021/acsami.1c09553>
- Bansal, B., & Chen, X. D. (2006). A Critical Review of Milk Fouling in Heat Exchangers. *Comprehensive Reviews in Food Science and Food Safety*, 5.
- Barone, G., Yazdi, S. R., Lillevang, S. K., & Ahm , L. (2021). Calcium: A comprehensive review on quantification, interaction with milk proteins and implications for processing of dairy products. *Comprehensive Reviews in Food Science and Food Safety*, 20(6), 5616–5640. <https://doi.org/10.1111/1541-4337.12844>
- Belmar-Beiny, M. T. and Fryer, P. J. (1993) Preliminary Stages of Fouling from Whey Protein Solutions, *Journal of Dairy Research*, 60(4), pp. 467–483
- Bennet, H. A. E. (2007). Aspects of fouling in dairy processing. Massey University, Palmerston North, 2007
- Benning, R., Petermeier, H., Delgado, A., Hinrichs, J., Kulozik, U., & Becker, T. (2003). Process Design for Improved Fouling Behavior in Dairy Heat Exchangers Using a Hybrid Modelling Approach. *Food and Bioprocess Processing*, 81(3), 266-274.
- Bouvier, L. et al. (2014) A CFD model as a tool to simulate  $\beta$ -lactoglobulin heat-induced denaturation and aggregation in a plate heat exchanger, *Journal of Food Engineering*. Elsevier, 136, pp. 56–63
- Boxler, C. (2014) *Fouling by Milk Constituents and Cleaning of Modified Surfaces*. Technischen Universit t Carolo-Whilhelmina zu Braunschweig.
- Boxler, Cristiane, Augustin, W. and Scholl, S. (2014) Composition of milk fouling deposits in a plate heat exchanger under pulsed flow conditions, *Journal of food engineering*. Elsevier, 121, pp. 1–8.
- Boxler, C, Augustin, W. and Scholl, S. (2014) Influence of surface modification on the composition of a calcium phosphate-rich whey protein deposit in a plate heat exchanger, *Dairy Science & Technology*. Springer, 94(1), pp. 17–31.
- Burton, H., Franklin, J.G., Williams, D.J., Chapman, H.R., Jean, A., Harrison, W., Clegg, L.F.L., 1959. An analysis of the performance of an ultra-high-temperature milk sterilizing plant: IV. Comparison of experimental and calculated sporicidal effects for a strain of *Bacillus stearothermophilus*. *J. Dairy Res.* 26, 221–226. doi:10.1017/S002202990000995X
- Dalgleish, D. G. (1990) Denaturation and aggregation of serum proteins and caseins in heated milk, *Journal of Agricultural and Food Chemistry*. ACS Publications, 38(11), pp. 1995–1999
- De Jong, P., Bouman, S., van der Linden, H.J.L.J. Fouling of heat treatment equipment in relation to the denaturation of  $\beta$ -lactoglobulin. *J. Soc. Dairy Techn.* 45(1992)3-8
- De Wit, J., Klarenbeek, G., 1989. Technological and functional aspects of milk proteins. *Milk Proteins*. Springer, pp. 211–222
- Eliaz, N., & Sridh, T. M. (2008). Electro crystallization of hydroxyapatite and its dependence on solution conditions. *Crystal Growth and Design*, 8(11), 3965–3977. <https://doi.org/10.1021/cg800016h>
- Gallot-Lavallee, T., Lalande, M., & Corrieu, G. (1984). Cleaning Kinetics Modeling of Holding Tubes Fouled During Milk Pasteurization. *Journal of Food Process Eng.* 7, 123–142
- Gillham, C. R., Fryer, P. J., Hasting, A. P. M., & Wilson, D. I. (1999). Cleaning-in-place of whey protein fouling deposits: Mechanisms Controlling Cleaning. *Food and Bioprocess Processing: Transactions of the Institution of Chemical Engineers*, Part C, 77(2), 127–136. <https://doi.org/10.1205/096030899532420>.
- Goode, K. R. et al. (2013) Fouling and cleaning studies in the food and beverage industry classified by cleaning type, *Comprehensive Reviews in Food Science and Food Safety*. Wiley Online Library, 12(2), pp. 121–143.
- Gu, Y., Bouvier, L., Tonda, A., & Delaplace, G. (2019). A mathematical model for the prediction of the whey protein fouling mass in a pilot scale plate heat exchanger. *Food Control*, 106, 106729.
- Jeurnink, T. J. M., & Brinkman, D. W. (1994). The cleaning of heat exchangers and evaporators after processing milk or whey. *International Dairy Journal*, 4(4), 347-368.
- Jeurnink, T. et al. (1996) Deposition of heated whey proteins on a chromium oxide surface, *Colloids, and surfaces B: Biointerfaces*. Elsevier, 6(4–5), pp. 291–307.
- Jimenez, M. et al. (2013) Toward the Understanding of the Interfacial Dairy Fouling Deposition and Growth Mechanisms at a Stainless-Steel Surface: A Multiscale Approach, *Journal of Colloid, and Interface Science*, 404, pp. 192–200. doi: <http://dx.doi.org/10.1016/j.jcis.2013.04.021>.
- Jun, S. and M. Puri, V. (2005) 3D Milk Fouling Model of Plate Heat Exchangers using Computational Fluid Dynamics. *St. Joseph, MI: ASAE (ASABE Paper No. 056063)*. doi: <https://doi.org/10.13031/2013.19600>.
- Jun, S., Puri, V., (2006). A 2D dynamic model for fouling performance of plate heat exchangers. *J. Food Eng.* 75, 364–374.

- Khalidi, M., Blanpain-Avet, P., Guérin R., Ronse G., L. Bouvier, André, C., Bornaz, S., Croguennec, T., Jeantet, R., Delaplace, G. (2015) Effect of Calcium Content and Flow Regime on Whey Protein Fouling and Cleaning in a Plate Heat Exchanger, *Journal of Food Engineering*, 147, pp. 68–78.
- Khalidi, Marwa. Etude du Lien entre la Physico chimie de Dérivés Laitiers et leur Aptitude à l'Encrassement Lors du Traitement Thermomécanique en Echangeur de Chaleur. Sciences de la Matière, du Rayonnement et de l'Environnement. Université des Sciences et Technologies (Lille 1). 2016. Français.
- Khalidi, M., Croguennec, T., André, C., Ronse, G., Jimenez, M., Bellayer, S., Blanpain-Avet, P., L. Bouvier, L. Six, T., Bornaz, S., R. Jeantet, R., Delaplace, G., (2018) Effect of the calcium/protein molar ratio on  $\beta$ -lactoglobulin denaturation kinetics and fouling phenomena, *International Dairy Journal*. Elsevier, 78, pp. 1–10.
- Lalande, M. and Rene, F. (1988) Fouling by Milk and Dairy Product and Cleaning of Heat Exchange Surfaces, in Melo, L. F., Bott, T. R., and Bernardo, C. A. (eds) *Fouling Science and Technology*. Springer Netherlands (NATO ASI Series), pp. 557–573.
- Liu, W., Chen, X. D., Jeantet, R., André, C., Bellayer, S., & Delaplace, G. (2021). Effect of casein/whey ratio on the thermal denaturation of whey proteins and subsequent fouling in a plate heat exchanger. *Journal of Food Engineering*, 289, 110175.
- Liu, W., Feng, Y., Delaplace, G., André, C., & Chen, X. D. (2022). Effect of calcium on the reversible and irreversible thermal denaturation pathway of  $\beta$ -lactoglobulin. *Food Hydrocolloids*, 133, 107943. <https://doi.org/10.1016/j.foodhyd.2022.107943>
- Lyster, R. L. J. (1965) The composition of milk deposits in an ultra-high-temperature plant, *Journal of Dairy Research*. Cambridge University Press, 32(2), pp. 203–208.
- Petit, J. et al. (2011) Influence of calcium on  $\beta$ -lactoglobulin denaturation kinetics: Implications in unfolding and aggregation mechanisms, *Journal of dairy science*. Elsevier, 94(12), pp. 5794–5810.
- Polat, Z. (2009) Integrated approach to whey utilization through natural zeolite adsorption/desorption and fermentation. İzmir Institute of Technology.
- Sadeghinezhad, E., Kazi, S.N., Dahari, M., Safaei, M.R., Sadri, R., Badarudin, A., (2014) A Comprehensive Review of Milk Fouling on Heated Surfaces, *Critical Reviews in Food Science and Nutrition*, 12(55), pp. 1724–1743.
- Scudeller, L.A., Blanpain-Avet, P., Six, T., Bellayer, S., Jimenez, M., Croguennec, T., André, C., Delaplace, G., 2021. Calcium chelation by phosphate ions and its influence on fouling mechanisms of whey protein solutions in a plate heat exchanger. *Foods* 10, 259.
- Skudder P.J., Thomas E.L., Pavey J.A., Perkin A.G. (1981) Effects of adding potassium iodate to milk before UHT treatment. I-Reduction in the amount of deposit on the heated surfaces. *Journal of Dairy Research* 48, 99–113,
- Spanos, N., Patis, A., Kanellopoulou, D., Andritsos, N., & Koutsoukos, P. G. (2007). Precipitation of calcium phosphate from simulated milk ultrafiltrate solutions. *Crystal Growth and Design*, 7(1), 25–29. <https://doi.org/10.1021/cg050361w>.
- Tuoc, T. K. (2015) 'Fouling in Dairy Processes', in. Amsterdam: Elsevier, pp. 533–556. doi: <http://dx.doi.org/10.1016/B978-0-444-63228-9.00020-6>
- Tung, M. S. (1998). Calcium Phosphates in Biological and Industrial Systems, p.52.
- Van Asselt, A., M. Vissers, F. Smit, and P. De Jong. 2005. In-line control of fouling. In Heat Exchanger Fouling and Cleaning—Challenges and Opportunities. Engineering Conferences International, Kloster Irsee, Germany
- Visser, J. and Jeurmink, T. J. M. (1997) Fouling of Heat Exchangers in the Dairy Industry, *Experimental Thermal and Fluid Science*, 14(4), pp. 407–424. doi: [http://dx.doi.org/10.1016/S0894-1777\(96\)00142-2](http://dx.doi.org/10.1016/S0894-1777(96)00142-2).
- Westhoff, D.C. (1978) Heating milk for microbial destruction: a historical outline and update. *J Food Protect* 41:122–130
- Wilson, D. I. (2018) Fouling during food processing—progress in tackling this inconvenient truth, *Current Opinion in Food Science*. Elsevier, 23, pp. 105–112
- Xiong, Y. L. (1992) Influence of pH and ionic environment on thermal aggregation of whey proteins, *Journal of Agricultural and Food Chemistry*. ACS Publications, 40(3), pp. 380–384.
- Zouaghi, S. (2018) Dairy fouling on stainless steel and design of antifouling surfaces. Lille 1.
- Zouaghi, S.; Frémiot, J.; André, C.; Grunlan, M. A.; Gruescu, C.; Delaplace, G.; Duquesne, S.; Jimenez, M. (2019) Investigating the Effect of an Antifouling Surface Modification on the Environmental Impact of a Pasteurization Process: An LCA Study. *ACS Sustainable Chem. Eng.* 2019, 7 (10), 9133–9142. <https://doi.org/10.1021/acssuschemeng.8b05835>